# Universal Criterion and Phase Diagram for Switching a Magnetic Vortex Core in Soft Magnetic Nanodots

Ki-Suk Lee,[1] Sang-Koog Kim,[1,*] Young-Sang Yu,[1] Youn-Seok Choi,[1] Konstantin Yu. Guslienko,[1] Hyunsung Jung,[1] and Peter Fischer[2]

[1]*Research Center for Spin Dynamics and Spin-Wave Devices, and Nanospinics Laboratory, Department of Materials Science and Engineering, Seoul National University, Seoul 151-744, Republic of Korea*

[2]*Center for X-Ray Optics, Lawrence Berkeley National Laboratory, 1 Cyclotron Road, Mail Stop 2R0400, Berkeley, California 94720, USA*

(Received 16 July 2008; revised manuscript received 14 October 2008; published 31 December 2008)

The universal criterion for ultrafast vortex-core switching between the up- and down-core bistates in soft magnetic nanodots is investigated by micromagnetic simulations along with vortex-core switching that occurs whenever the velocity of vortex-core motion reaches its critical velocity, $v_{cri} = (1.66 \pm 0.18)\gamma\sqrt{A_{ex}}$ (e.g., $v_{cri} = 330 \pm 37$ m/s for Permalloy), with the exchange stiffness $A_{ex}$ and the gyromagnetic ratio $\gamma$. On the basis of the universality of $v_{cri}$, phase diagrams for the vortex-core switching event and switching time with respect to both the amplitude and frequency of a circularly rotating magnetic field are calculated.

DOI: 10.1103/PhysRevLett.101.267206 PACS numbers: 75.40.Gb, 75.40.Mg, 75.60.Jk, 75.75.+a

In magnetic thin films [1,2] and patterned elements of micrometer (or smaller) lateral size [3], a nonuniform magnetization (**M**) configuration has been experimentally observed in both static and dynamic states. This magnetic nanostructure, the so-called ''magnetic vortex (MV),'' has an in-plane curling **M** along with an out-of-plane **M** at the core of a few tens of nm size [3]. Owing to a high thermal stability of the bistate **M** orientations of the tiny vortex core (VC), the MV has received considerable attention as the information carrier of binary digits ''0'' and ''1'' in future nonvolatile memory devices [4]. Furthermore, very recently experimental, theoretical, and simulation studies have explored a rich variety of the dynamic properties of the MV, including ultrafast VC switching by linearly oscillating [5–7] and circularly rotating [8–10] in-plane magnetic fields or spin-polarized ac currents [11,12], with extremely low-power consumption. The underlying mechanism and physical origin of ultrafast VC switching have also been found [5–7,13]. These rich dynamic properties stimulate continuing intensive studies of patterned magnetic elements in vortex states targeting towards a fundamental understanding of their dynamics [6,7,11,13,14] and practical applications to a new class of nonvolatile random access memory [15] and patterned memory media [4,9]. Such new conceptual devices have become emerging key issues in the research areas of nanomagnetism and **M** dynamics. Although the fundamental understanding of the VC reversal and vortex gyrotropic dynamics were much advanced recently, the universal criterion for VC switching, its phase diagram, and switching time have not been investigated yet. Moreover, these are technologically essential parameters for a reliable manipulation of the VC switching acting as a basic function in memory devices, which should be identified for its practical applications.

In this Letter, we report on the universal criterion, the critical velocity $v_{cri}$ of VC motions required for VC switching, as found by micromagnetic simulations and analytical calculations. On the basis of the universality of $v_{cri}$ we derive phase diagrams of the VC reversal event and switching times with respect to the amplitude and frequency of *circularly rotating* magnetic fields.

In the present study, the OOMMF code [16] was used that utilizes the Landau-Lifshitz-Gilbert equation of motion [17] because this approach is a well established, optimized tool to investigate **M** dynamics on a few nm spatial and 10 ps temporal scales. In addition, we used an analytical approach to determine the threshold of driving forces required for VC switching and the necessary switching times based on the linearized Thiele's equation [18]. We used Permalloy (Py: $Ni_{80}Fe_{20}$) nanodots as a model system, and the Gilbert damping parameter $\alpha = 0.01$, each dot with a different radius $R$ ranging from 150 to 600 nm and a different thickness $L$ ranging from 10 to 50 nm [see Fig. 1(a)].

To excite vortex gyrotropic motions up to the VC switching, we used specially designed counter-clockwise (CCW) circularly rotating magnetic fields in the dot plane with the angular frequency $\omega_{\mathbf{H}}$ and the amplitude $H_0$, denoted as $\mathbf{H}_{CCW} = H_0[\cos(\omega_{\mathbf{H}}t)\hat{\mathbf{x}} + \sin(\omega_{\mathbf{H}}t)\hat{\mathbf{y}}]$ [19,20]. The reason for selecting this $\mathbf{H}_{CCW}$ is that it is most effective for selective resonant excitations of only the core-up vortex state, as demonstrated in earlier theoretical and simulation works [9,20], and in recent experimental work [10]. An example of the resonant vortex gyrotropic motion and VC switching driven by $\mathbf{H}_{CCW}$ with $H_0 = 20$ Oe and $\nu_{\mathbf{H}} = \omega_{\mathbf{H}}/2\pi = \nu_D = 580$ MHz (where $\nu_D$ is the vortex eigenfrequency) [21,22] is shown in supplementary Fig. 1 in [23]. It is numerically found that the up-

 

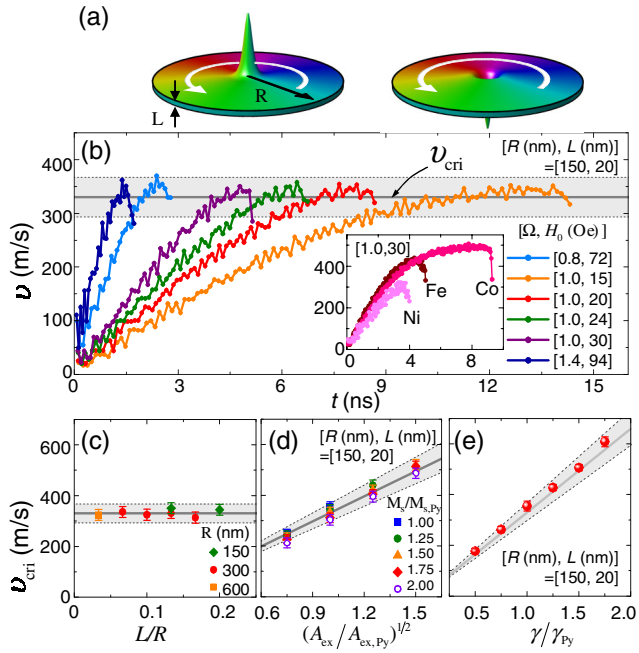


FIG. 1 (color online). (a) Magnetic vortex structure with either upward or downward core **M** orientation. The rotation sense of the local in-plane **M** around the VC is CCW. (b) Instantaneous VC velocity $v(t)$ in the Py dot of $R = 150$ nm and $L = 20$ nm for different values of $H_0$ and $\Omega = \omega_{\mathbf{H}}/\omega_D$. The inset shows the VC velocities versus time for different dots made of Fe, Co, and Ni. (c), (d), and (e) show the dependences of $\upsilon_{cri}$ on the dimensions of the Py dot, the material parameters of $A_{ex}$, $M_s$, and $\gamma$, respectively. All the results were obtained from the micromagnetic simulations. The gray-colored regions with the lines indicate the value of $\upsilon_{cri}$ with its error range $\pm 37$ m/s.

core switches to the down core when the velocity of the up-core motion reaches a threshold velocity, $\upsilon_{cri}^{Py} = 330$ m/s for the Py dot, as seen in the right panel of supplementary Fig. 1 in [23], and in our earlier works [9,12,13].

To examine the universality of $\upsilon_{cri}^{Py} = 330$ m/s, we conducted additional simulations to obtain the VC velocity-versus-time curves varying both $H_0$ (10 to 350 Oe) and $\nu_{\mathbf{H}}$ (0.1 to 2 GHz) for a Py dot of $R = 150$ nm and $L = 20$ nm, as shown in Fig. 1(b). It is established that the value of $\upsilon_{cri}^{Py} = 330 \pm 37$ m/s is neither affected by the external field parameters of $\nu_{\mathbf{H}}$ and $H_0$ nor by the size of the Py dot, as evidenced by the independence of $\upsilon_{cri}$ on the dot radius and thickness [Fig. 1(c)]. Furthermore, in order to examine whether any of the intrinsic material parameters affect the value of $\upsilon_{cri}^{Py}$, we performed simulations for a circular dot of $R = 150$ nm and $L = 20$ nm, according to artificially varying $M_s$ (the saturation magnetization), $A_{ex}$, and $\gamma$ (the gyromagnetic ratio) [24]. The simulation results in Figs. 1(d) and 1(e) display a linear increase of $\upsilon_{cri}$ with $(A_{ex}/A_{ex,Py})^{1/2}$ with an equal slope for different values of $M_s$, and a linear increase with $\gamma/\gamma_{Py}$, respectively ($\upsilon_{cri}$ dependence on $\alpha$ is also shown in supplementary Fig. 2 in [23]).

All the simulation results confirm an explicit analytical form of $\upsilon_{cri} \simeq \eta\gamma\sqrt{A_{ex}}$ with the proportional constant $\eta = 1.66 \pm 0.18$. To check the universality of this constant for different magnetic materials, we also simulated the VC switching with Ni, Fe, and Co, as shown in the inset of Fig. 1(b) [25]. All $\eta$ values for the different materials are close to 1.66 and thus identical within the estimated errors. The $\eta = 1.66$ acts as a universal constant that relates $\upsilon_{cri}$, and only $A_{ex}$ and $\gamma$. It is also interesting that $\upsilon_{cri} \simeq 1.66\gamma\sqrt{A_{ex}}$ does not explicitly include $M_s$. This fact can be understood from the physical origin of the VC switching, the gyrofield, as reported previously [13]. The dominant contribution to the critical gyrofield is the short-range exchange interaction. Therefore, $A_{ex}$ is the dominant parameter in determining the critical gyrofield and in turn $\upsilon_{cri}$. Following the same argument, the long-range dipolar interaction gives a negligible contribution to $\upsilon_{cri}$, so that the dimensions and shape of a given dot, as well as $M_s$ do not affect the value of $\upsilon_{cri}$, as manifested itself in the equation, $\upsilon_{cri} \simeq 1.66\gamma\sqrt{A_{ex}}$.

On the basis of the universality of $\upsilon_{cri}$, we construct phase diagrams of the VC switching criterion and switching times with respect to $\omega_{\mathbf{H}}$ and $H_0$. Figure 2 shows the simulation results on the switching boundary diagram, where the VC switching (light gray) and nonswitching (white) areas are differentiated by different symbols for different dimensions, $[R(\text{nm}), L(\text{nm})] = [150, 20]$, $[150, 30]$, $[300, 20]$, and $[450, 20]$. The switching event boundaries for all the different dot dimensions form almost the same line, which reflects again the fact that $\upsilon_{cri}$ does not vary with the size of a given dot. Owing to the resonant excitation of VC motions at $\omega_{\mathbf{H}} = \omega_D$, the VC velocity can reach $\upsilon_{cri}$ through its gyrotropic motion although it is

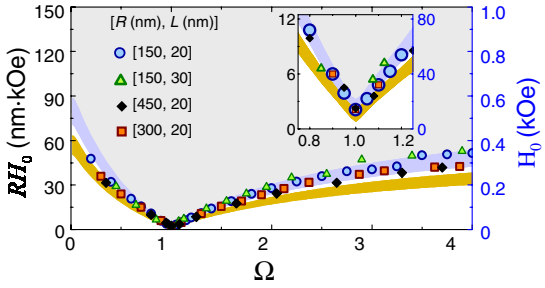


FIG. 2 (color online). The boundary diagram of the VC switching driven by the field $\mathbf{H}_{CCW}$ in the $\Omega - RH_0$ plane. Blue circle, green triangle, orange square and black diamond symbols correspond to the simulated results for $[R(\text{nm}), L(\text{nm})] = [150, 20]$, $[150, 30]$, $[300, 20]$, and $[600, 20]$, respectively. The yellow (dark gray) colored area indicates the switching boundary obtained using the analytical equation of $RH_0^C$ shown in the text for Py dots with $R = 50$–$5000$ nm and $L = 20$–$80$ nm, based on the estimated value of $\upsilon_{cri}^{Py} = 330 \pm 37$ m/s. The light purple (gray) colored area is the result of the multiplication of $S_F = 1.4$ to the equation of $RH_0^C$. The right side (blue-colored) axis indicates the result corresponding to specific dimensions, $[R(\text{nm}), L(\text{nm})] = [150, 20]$.

driven by extremely small $H_0$ values [5,9,10]. Resonant VC motions yield a deep valley on the switching boundary in the vicinity of $\omega_{\mathbf{H}} = \omega_D$, and, thus, the threshold value of $H_0$ required for the VC switching has a minimum at $\omega_{\mathbf{H}} = \omega_D$.

In addition, we theoretically derived explicit analytical equations representing the switching boundary, which distinguishes the event of the VC switching and nonswitching based on the linearized Thiele's equation. A detailed derivation is described in Ref. [23]. Here we chose $\mathbf{H}_{\mathrm{CCW}}$ necessary for the resonant gyrotropic motion of the up-core and successive core switching to the down core [9,10,20]. From the general solution of the equation of VC motion in the linear regime, the instantaneous velocity of the up-core motion as a function of time $t$ driven by $\mathbf{H}_{\mathrm{CCW}}$ is found as $v(t) = \frac{1}{3}\gamma R H_0 \sqrt{\Omega^2 + F(\Omega, t)}/\sqrt{(1-\Omega)^2 + d^2\Omega^2}$, where $d = -D/|G|$, $G = 2\pi L M_s/\gamma$ is the gyrovector constant, $D < 0$ is the damping constant [18], and $\Omega = \omega_{\mathbf{H}}/\omega_D$. The function $F(\Omega, t)$ represents the time variable velocity term of the transient VC motions and has a maximum at $t_m \approx \pi/|\omega_{\mathbf{H}} - \omega_D|$ [23]. This $v(t)$ in turn allows us to analytically construct the VC switching boundary ($RH_0^C$) diagram in the $\Omega - RH_0$ plane by putting $v(t) = v_{\mathrm{cri}}$ and $H_0 = H_0^C$, as written by $RH_0^C \approx (3v_{\mathrm{cri}}/\gamma) \times \sqrt{(1-\Omega)^2 + d^2\Omega^2}/(\Omega + e^{-d\omega_D t_m})$. The numerical calculation of $RH_0^C(\Omega)$ using $v_{\mathrm{cri}}^{\mathrm{Py}} = 330 \pm 37$ m/s is displayed by the yellow- (dark gray-) colored area in Fig. 2. At $\Omega = 1$, the minimum value of $RH_0^C$ is $3dv_{\mathrm{cri}}/\gamma$, where $d = \alpha[1 + \ln(R/R_c)/2]$, $R_c$ is the VC radius [26], indicating that $H_0^C(\Omega = 1) \sim 3dv_{\mathrm{cri}}/\gamma R$ is the lowest field strength required for the VC switching [27]. The analytical solution [yellow- (dark gray-) colored area] is somewhat in discrepancy with the micromagnetic simulations (symbols), although they are similar in shape or trend. This discrepancy can be associated with the fact that the present simulations of the VC switching imply a nonlinearity of the VC gyrotropic motions when the motions are close to the switching event [28], whereas the above analytical equation of $RH_0^C$ assumes only linear-regime vortex motions. However, this nonlinear effect could be compensated simply by multiplying a scaling factor $S_F = +1.4$ to the above equation of $RH_0^C$. Recent experimental results by Curcic *et al.* [10] support our predicted value of $H_0^C$. Their reported value of $H_0^C = 3.4$ Oe for a square dot of 500 nm width and 50 nm thickness [10] is in good agreement with our value $H_0^C = 4.1$ Oe, obtained from $S_F 3dv_{\mathrm{cri}}/\gamma R$ for $\Omega = 1$, considering their system dimensions and experimentally measured value, $v_{\mathrm{cri}}^{\mathrm{Py}} = 190$ m/s, although this value is much smaller than our simulation value, $330 \pm 37$ m/s [29].

Next, we construct a phase diagram of the switching time $T_S$, i.e., the time period necessary for the VC switching to complete itself. As already reported in Ref. [7], the VC switching occurs through the serial processes of the nucleation and annihilation of a vortex-antivortex (V-AV) pair around the initial VC position, following the maximum deformation of the entire VC **M** structure [7,13]. This process follows just after $v(t)$ reaches $v_{\mathrm{cri}}$ through the gyrotropic motion [12]. Accordingly, $T_S$ consists of three different duration times, $T_S = \Delta t_g + \Delta t_d + \Delta t_{\text{V-AV}}$. The individual times can thus be determined by the three different processes: $\Delta t_g$, the time period required for a VC to reach $v_{\mathrm{cri}}$; $\Delta t_d$, the time period after that, and until a V-AV pair is nucleated; and $\Delta t_{\text{V-AV}}$, the time period during which the serial processes of the nucleation and annihilation of the V-AV pair occur until the VC switching is completed. To estimate each value of $\Delta t_g$, $\Delta t_d$, $\Delta t_{\text{V-AV}}$, the above indicated successive processes are differentiated according to the definition of each process, as shown in micromagnetic simulations for a Py dot of $R = 150$ nm and $L = 20$ nm (for details, see Ref. [23]). Then, each value of $\Delta t_g$, $\Delta t_d$, $\Delta t_{\text{V-AV}}$, and $T_S$ are plotted as a function of $H_0$ in Fig. 3(a). For $H_0 < 0.4$ kOe, $\Delta t_g$ is on the order of a few ns and becomes increased with decreasing $H_0$. Note that $\Delta t_g$ is much longer than both $\Delta t_d$ ($\sim 50$ ps) and $\Delta t_{\text{V-AV}}$ ($\sim 30$ ps). For $H_0 > 0.5$ kOe, however, $\Delta t_g$ reaches a few ps, being much less than $\Delta t_d$ and $\Delta t_{\text{V-AV}}$, according to the simulation results. However, the Landau-Lifshitz-Gilbert equation of motion used in the simulations is invalid below 1 ps time scale, so that all the results below 1 ps (10 ps as an upper bound) are physically meaningless. Consequently, there is no doubt that for $H_0 < 0.4$ kOe, $T_S$ can be approximately determined by $\Delta t_g$, whereas for $H_0 > 0.5$ kOe, $T_S$ is determined by the sum of $\Delta t_d$ and $\Delta t_{\text{V-AV}}$, i.e., at least $\sim 80$ ps, only in the range of physically meaningful switching time. From an application point of view, such high field strengths are not necessary for the VC switching when applying the resonance frequency. In other words, in the range of $H_0 < 0.4$ kOe, $\Delta t_g$ is sufficient to represent $T_S$. $\Delta t_g$ can also be calculated simply using the analytical equation of $v(t)$ along with the

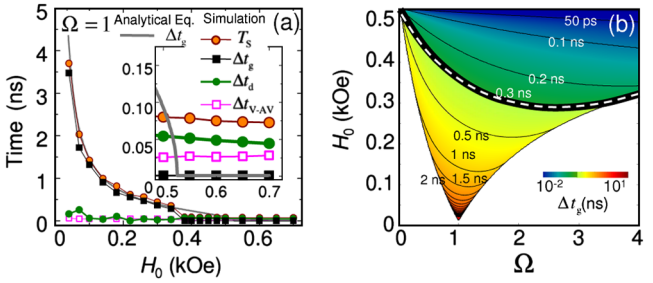


FIG. 3 (color online). (a) Time periods for the individual indicated processes as a function of the amplitude $H_0$ of $\mathbf{H}_{\mathrm{CWW}}$ at $\omega_{\mathbf{H}}/2\pi = \omega_D/2\pi = 580$ MHz, obtained from micromagnetic simulations (symbols with lines) for a Py dot of $R = 150$ nm and $L = 20$ nm, being compared with the numerical calculation (line) of the analytical form of $\Delta t_g$. (b) Contour plot of the VC switching time in the $\Omega - H_0$ plane, obtained from the numerical calculation of $\Delta t_g$ for the Py dot with $R = 150$ nm and $L = 20$ nm. $\Delta t_g$ only in the region below the indicated white dashed line determines $T_S$.

condition $v(t) = v_{cri}$ at $t = \Delta t_g$ and taking into account the nonlinear effects that can be also compensated by the scaling factor $S_F$. For $\Omega = 1$ and $H_0 > H_0^C$ (nonswitching for $H_0 < H_0^C$), $\Delta t_g$ is analytically expressed as $\Delta t_g(H_0) = -(d\omega_D)^{-1} \ln(1 - H_0^C/H_0)$, and this numerical solution is compared with the simulation result in Fig. 3(a).

For $\Omega \neq 1$, $\Delta t_g$ can also be numerically calculated, as shown in Fig. 3(b), e.g., for a Py dot of $R = 150$ nm and $L = 20$ nm. For $H_0 \gg H_0^C$, $\Delta t_g$ is $\sim$1 ps, and does not vary much with $\omega_{\mathbf{H}}$, but this time scale is physically meaningless, as already mentioned. In contrast, as $H_0$ decreases close to $H_0^C$, $\Delta t_g$ markedly increases and varies considerably with $\omega_{\mathbf{H}}$. At $\Omega = 1$, it appears that the lower the $H_0^C$, the longer the $\Delta t_g$ [30]. For faster VC switching, larger values of $H_0$ and $\omega_{\mathbf{H}} > \omega_D$ are more effective. Since $\Delta t_g$ of $\sim$1 ps for $H_0 > 0.5$ kOe is not meaningful any more, and in such higher field region only $\Delta t_d + \Delta t_{\text{V-AV}}$ determines $T_S$, only the region of $H_0 < 0.4$ kOe or $\Delta t_g > 0.3$ ns in the phase diagram, shown in Fig. 3(b), would be technologically useful in the optimization of driving force parameters that reliably control the ultrafast VC switching.

In conclusion, $v_{cri} = 1.66\gamma\sqrt{A_{ex}}$ has been found to serve as the universal criterion for VC switching, e.g., $v_{cri}^{Py} = 330 \pm 37$ m/s. Based on this criterion, we derived phase diagrams of the VC switching and the switching time with respect to the frequency and amplitude of the circularly rotating field, which provide guidance for practical implementations of a dot array in the vortex states to information storage devices. These phase diagrams are also useful in the design of the dot dimensions and proper choice of materials as well as to optimize external driving forces for the reliable ultrafast VC switching at extremely low-power consumption.

We thank H. Stoll for fruitful discussions. This work was supported by Creative Research Initiatives (ReC-SDSW) of MEST/KOSEF. P. F. was supported by the Director, Office of Science, Office of Basic Energy Sciences, Materials Sciences and Engineering Division, of the U.S. Department of Energy.

*To whom all correspondence should be addressed.
sangkoog@snu.ac.kr

[1] A. Hubert and R. Schäfer, *Magnetic Domains* (Springer-Verlag, Berlin, 1998).
[2] S.-K. Kim, J. B. Kortright, and S.-C. Shin, Appl. Phys. Lett. **78**, 2742 (2001); S.-K. Kim *et al.*, Appl. Phys. Lett. **86**, 052504 (2005).
[3] T. Shinjo *et al.*, Science **289**, 930 (2000); A. Wachowiak *et al.*, Science **298**, 577 (2002); J. Miltat and A. Thiaville, Science **298**, 555 (2002).
[4] R. P. Cowburn, Nature Mater. **6**, 255 (2007); J. Thomas, Nature Nanotech. **2**, 206 (2007).
[5] B. Van Waeyenberge *et al.*, Nature (London) **444**, 461 (2006).
[6] R. Hertel *et al.*, Phys. Rev. Lett. **98**, 117 201 (2007); Q. F. Xiao *et al.*, J. Appl. Phys. **102**, 103904 (2007).
[7] K.-S Lee *et al.*, Phys. Rev. B **76**, 174410 (2007).
[8] V. P. Kravchuk *et al.*, J. Appl. Phys. **102**, 043908 (2007).
[9] S.-K. Kim *et al.*, Appl. Phys. Lett. **92**, 022509 (2008).
[10] M. Curcic *et al.*, Phys. Rev. Lett. **101**, 197204 (2008).
[11] K. Yamada *et al.*, Nature Mater. **6**, 270 (2007).
[12] S.-K. Kim *et al.*, Appl. Phys. Lett. **91**, 082506 (2007).
[13] K. Y. Guslienko, K.-S. Lee, and S.-K. Kim, Phys. Rev. Lett. **100**, 027203 (2008).
[14] B. Krüger *et al.*, Phys. Rev. B **76**, 224426 (2007); M. Bolte *et al.*, Phys. Rev. Lett. **100**, 176601 (2008).
[15] S.-K. Kim *et al.*, IEEE Trans. Magn. 44, 3071 (2008).
[16] See http://math.nist.gov/oommf.
[17] L. D. Landau and E. M. Lifshitz, Phys. Z. Sowjetunion **8**, 153 (1935); T. L. Gilbert, Phys. Rev. **100**, 1243 (1955).
[18] A. A. Thiele, Phys. Rev. Lett. **30**, 230 (1973); D. L. Huber, Phys. Rev. B **26**, 3758 (1982).
[19] A linearly oscillating field can be decomposed into the CCW and clockwise (CW) rotating fields with the equal $H_0$ and $\omega_{\mathbf{H}}$ values [9].
[20] K.-S. Lee and S.-K. Kim, Phys. Rev. B **78**, 014405 (2008).
[21] K. Y. Guslienko *et al.*, J. Appl. Phys. **91**, 8037 (2002).
[22] J. P. Park *et al.*, Phys. Rev. B **67**, 020403 (2003); S. B. Choe *et al.*, Science **304**, 420 (2004); K. Y. Guslienko *et al.*, Phys. Rev. Lett. **96**, 067205 (2006).
[23] See EPAPS Document No. E-PRLTAO-102-058902 for supplementary documents for (a) the derivation of instantaneous VC velocity, $v(t)$ and (b) the entire switching time $T_S$ for complete vortex-core switching. For more information on EPAPS, see http://www.aip.org/pubservs/epaps.html.
[24] We used $M_s/M_{s,\text{Py}} = 1.0$–$2.0$, $(A_{ex}/A_{ex,\text{Py}})^{1/2} = 0.75$–$1.5$, and $\gamma/\gamma_{\text{Py}} = 0.5$–$1.75$, where $M_{s,\text{Py}} = 860$ emu/cm$^3$, $A_{ex,\text{Py}} = 1.3$ $\mu$erg/cm, $\gamma_{\text{Py}} = 2.8 \times 2\pi$ MHz/Oe for Py.
[25] For Fe, Co, and Ni, $A_{ex} = 2.1$, 3.0, and 0.9 $\mu$erg/cm, $M_s = 1700$, 1400, 490 emu/cm$^3$ were used, respectively, with the same value of $\gamma = 2.8 \times 2\pi$ MHz/Oe. In the literature, different values for those material parameters are used. The values of $\eta_{\text{Fe}} = 1.72 \pm 0.09$, $\eta_{\text{Co}} = 1.66 \pm 0.06$, and $\eta_{\text{Ni}} = 1.91 \pm 0.24$ for these materials are obtained using the corresponding critical velocities, $v_{cri}^{\text{Fe}} = 439 \pm 22$, $v_{cri}^{\text{Co}} = 507 \pm 19$, $v_{cri}^{\text{Ni}} = 320 \pm 40$ m/s.
[26] K. Y. Guslienko, Appl. Phys. Lett. **89**, 022510 (2006).
[27] For CW rotating fields, $RH_0^C$ has a constant value of $3v_{cri}/\gamma$, which indicates that the $RH_0^C$ value of the $\mathbf{H}_{\text{CW}}$ is much larger than that of $\mathbf{H}_{\text{CWW}}$.
[28] K.-S. Lee and S.-K. Kim, Appl. Phys. Lett. **91**, 132511 (2007); K. S. Buchanan *et al.*, Phys. Rev. Lett. **99**, 267201 (2007).
[29] In contrast to micromagnetic simulation results on an ideal system, the experimental values of $v_{cri}$ may be affected by other factors such as measurement errors, and the imperfections (nonmagnetic defects, grain boundaries, edge roughness) and different material parameters of real samples.
[30] From micromagnetic simulation results for $R = 150$ nm (300 nm) and $L = 20$ nm, $H_0^C$ is only 14 Oe (7 Oe) and $T_S$ is 17 ns (33 ns).